

Effect of hydrodynamic interactions on rapid Brownian coagulation of colloidal dispersionsYuki Matsuoka,^{1,*} Tomonori Fukasawa,² Ko Higashitani,² and Ryoichi Yamamoto^{2,†}¹*Production Engineering Research Laboratory, Sumitomo Bakelite Co., Ltd., Shizuoka 426-0041, Japan*²*Department of Chemical Engineering, Kyoto University, Kyoto 615-8510, Japan*

(Received 19 July 2012; published 14 November 2012)

The rate of rapid Brownian coagulation is investigated for dispersions of spherical particles with particle volume fractions ranging from $\phi_p = 0.003$ to 0.1 by the direct numerical simulation method. This method explicitly considers hydrodynamic interactions (HIs) between particles by simultaneously solving for the motions of the dispersed particles and the host fluid. In the dilute limit, the rate of rapid Brownian coagulation decreases to approximately 0.3–0.5 times the theoretical Smoluchowski rate. We compare this result with results of previously reported experiments and theoretical predictions and find a strong correlation between them. This demonstrates that HIs between particles significantly reduce the coagulation rate. Moreover, the volume fraction dependence of the coagulation rate indicates that the coagulation rate increases with increasing volume fraction. At high particle volume fractions, the initial coagulation stage is affected by heterogeneous coagulation process before the steady state is reached.

DOI: [10.1103/PhysRevE.86.051403](https://doi.org/10.1103/PhysRevE.86.051403)

PACS number(s): 82.70.-y, 82.20.Wt, 83.10.Pp, 61.43.Hv

I. INTRODUCTION

Since Smoluchowski developed his theory of the Brownian coagulation process in colloidal dispersions based on population balance equations of coagulates and coagulation kinetics [1], many theoretical, experimental, and simulation studies have investigated the validity of this theory. A major deficiency of the Smoluchowski theory is that it predicts a coagulation rate that is approximately twice as large as the actual coagulation rate of colloidal dispersions [2–6]. This discrepancy has been mainly attributed to the theory's failure to consider interparticle interactions. Thus, a correction factor for the coagulation rate that considers interparticle interactions (hydrodynamic lubrication, Derjaguin-Landau-Verwey-Overbeek interaction [7,8], etc.) has been proposed [9–11]. Many experimental examinations of this correction have been conducted [2–6,12]. It has been suggested that the lower observed aggregation rate is due mostly to hydrodynamic lubrication forces between particles that hinder two particles approaching each other. However, these experimental examinations depend on the proposed correction factor itself. Consequently, evaluation of the hydrodynamic term in the correction factor is replaced by evaluation of other interparticle interactions, such as Van der Waals attractions. Thus, additional direct evaluations of these hydrodynamic effects would be valuable.

In the Smoluchowski formalism, particles are assumed to be spherical and the coagulation process is limited to simple two-body collisions between coagulates of the same size. These assumptions are only valid in the early stages of coagulation in dilute dispersions. In addition to the coagulation process itself, the formation of fractal structures in the coagulate clusters significantly affects the coagulation rate in the later stages of coagulation. An increase in the coagulation rate in the later stages of coagulation is observed experimentally. A theory of coagulation kinetics that is applicable to the later stages

of coagulation has been proposed. This model considers the steric effect of coagulation on the coagulation rate [13,14].

The coagulation rate is known to be enhanced in the very early stages of coagulation in which the spatial distribution of particles has not yet reached a steady state [1,15]. As the volume fraction of dispersed particles increases, the characteristic coagulation time (i.e., the time for the initial particle number to be halved) becomes shorter. At a certain volume fraction, the coagulation time becomes comparable to the transition period in which the effects of the unsteady state are significant. Therefore, coagulation times at higher volume fractions are greatly affected by the effects of the unsteady state. An increase in the coagulation rate at high particle volume fractions has been experimentally observed [3]. However, a detailed mechanism for this enhancement in the coagulation rate has yet to be elucidated.

Computer simulations are potentially superior to physical experiments for investigating these problems since simulations avoid difficulties such as preparing an initial dispersed particle distribution and observing aggregate forms at high concentrations. They can thus provide essential insights that can be used to evaluate proposed theories. Several simulations of colloidal coagulation have been reported, including some that employ Brownian dynamics (BD) and Langevin dynamics (LD) [14,16–19]. In these simulations, the coagulation rate has been observed to increase with increasing particle volume fraction [14,16–18]. Lattuada recently proposed a correction to the Smoluchowski equation for high volume fractions by using a result derived from trapping theory for the diffusion-limited reaction of chemical species. His theory and results appear to be consistent when assessed by a BD simulation [19].

The BD and LD simulation methods are effective for calculations of large systems because they have low computational costs. However, their handling of hydrodynamic interactions (HIs), such as lubrication forces, that act between particles is inadequate and may give rise to significant discrepancies between calculation and experimental results. This is especially true for colloidal particles dispersed in viscous liquids, such as water, solvents, or resins. In particular, simulations performed without considering HIs (such as the

*ymatsuoka@sumibe.co.jp

†ryoichi@cheme.kyoto-u.ac.jp

BD method) yield coagulation rates in the dilute limit that are very similar to the theoretical value given by the Smoluchowski theory, which does not consider HIs. Although BD simulations with average hydrodynamic corrections have recently been conducted, a reduction in the coagulation rate such as that found in experiments at low volume fractions was not observed [18].

Brady and Bossis developed the Stokesian dynamics (SD) simulation method that correctly incorporates hydrodynamic effects in the low Re limit [20]. The SD method represents short-range lubrication forces and long-range hydrodynamic forces by the sum of two-body analytic interactions. This method has been adapted to the rheology of colloidal dispersions and sedimentation phenomena in which fluid hydrodynamics significantly affect particle dynamics [20,21]. Although the SD method has provided much valuable information regarding these phenomena, the assumption that HIs can be treated as the sum of two-body interactions fails to consider many-body HIs, which may be important in coagulation of high volume fractions [22,23]. Consequently, to gain a complete understanding of these coagulation processes, it is desirable to consider many-body HIs.

In recent years, several numerical methods have been developed that accurately simulate dispersion in a variety of situations, including those described above [22,24–27]. These dispersion modeling techniques are all based on the same approach that involves determining fluid motion simultaneously with particle motion. We refer to this approach as the direct numerical simulation (DNS) approach. This approach enables us to accurately consider full time-dependent many-body HIs. In this study, we apply a direct numerical scheme based on the smoothed profile (SP) method [24] to a monodisperse dispersion of neutrally buoyant attractive Brownian particles in a stationary fluid. In SP method, the Navier-Stokes equation for the fluid motion is discretized on a regular grid and Newton's equations for particle motion are solved simultaneously with fluid motion.

In the present study, we examine the rate of rapid Brownian coagulation for a low particle volume fraction $\phi_p = 0.003$ and for a relatively high volume fraction $\phi_p = 0.1$ using the DNS method, which accurately accounts for HIs. Specifically, we focus on whether our simulation gives a lower coagulation rate from that predicted by the Smoluchowski theory. Because our simulation explicitly considers full many-body HIs, successful reproduction of the reduced coagulation rate would imply that the reduction is due to hydrodynamic effects. In addition, the volume fraction dependence of the coagulation rate is investigated. In these analyses, the focus is mainly on early stage of coagulations. However, at high particle volume fractions, our results show deviations from the early time behavior. Some interpretations to this effect will be given as well.

II. KINETIC THEORY OF RAPID COAGULATION

In general, the kinetic equation of Brownian coagulation is given by

$$\frac{dn_k}{dt} = \frac{1}{2} \sum_{i=1, i+j=k}^{i=k-1} \beta(i, j) n_i n_j - \sum_{i=1}^{\infty} \beta(k, i) n_k n_i, \quad (1)$$

where n_k is the concentration of particles with size k at time t and $\beta(i, j)$ is the collision frequency factor between particles with sizes i and j . Since the collision frequency factor depends on the individual properties of a particular motion and on particle interactions, its functional form is generally unknown except for some ideal cases. Once the collision frequency factors and initial conditions have been determined, it is possible to obtain information about the coagulation rates and cluster size distributions during coagulation by solving the simultaneous equations Eq. (1) for each cluster size. Smoluchowski considered particle collisions in terms of the relative diffusion of one particle with respect to another and showed that a simple form of the collision frequency factor in the early stages of coagulation of initially monodisperse suspensions could be determined by solving the diffusion equation in spherical coordinates [1]. The particle spatial distribution of i -fold clusters around j -fold clusters $n_i(r, t)$ and the collision frequency factor $\beta(i, j)$ are expressed by

$$n_i(r, t) = n_i(t) \left(1 - \frac{R_{ij}}{r} + \frac{2R_{ij}}{\sqrt{\pi r}} \int_0^{\frac{r-R_{ij}}{\sqrt{4D_{ij}t}}} e^{-\xi^2} d\xi \right), \quad (2)$$

$$\beta(i, j) n_i(t) = 4\pi R_{ij}^2 D_{ij} \left(\frac{\partial n_i}{\partial r} \right)_{r=R_{ij}} \quad (3)$$

$$= 4\pi R_{ij} D_{ij} n_i(t) \left(1 + \frac{R_{ij}}{\sqrt{\pi D_{ij}t}} \right), \quad (4)$$

where r is the distance between the two clusters and $n_i(t) = n_i(\infty, t)$, $R_{ij} = R_{c,i} + R_{c,j}$, $D_{ij} = D_i + D_j$, where $R_{c,i}$, D_i are the collision radius and the translational diffusion constant of the cluster with size i , respectively. The last term in Eq. (4) represents the unsteady effect that increases the coagulation rate during the initial stages of coagulation. This effect reflects the unsteady state of the particle spatial distribution from the beginning of coagulation to the establishment of a steady-state particle distribution. The time dependence of the particle spatial distribution expressed by Eq. (2) is shown in Fig. 1. Equation (2) assumes a spatially uniform particle distribution as the initial condition. As coagulation starts and proceeds, i -fold clusters diffuse toward j -fold clusters, leading to collisions and a subsequent reduction in the density near j -fold clusters. Accordingly, $\sim R_{ij}^2/D_{ij}$, the gradient of particle distribution at $r/R_{ij} = 1$ is often steep and the particle flux becomes large. At later times, the area with reduced density extends to larger interparticle distances. Ultimately, little further change in the particle distribution occurs and a steady-state particle distribution, $n_i(r, t) = n_i(t)(1 - R_{ij}/r)$, is established. In our case, the initial particle distribution is not uniform, particularly at high volume fractions. In addition, interparticle interactions due to HIs and direct interparticle interactions may alter the time dependence of the particle distribution. The unsteady effects on the coagulation rate are expected to be more complicated than was proposed by Smoluchowski. These complex initial conditions or boundary conditions in the diffusion equation have been studied, especially in the field of the kinetics of chemical reactions in solution [28].

Assuming that the Stokes-Einstein relation, $D_i = k_B T / 6\pi\mu R_{H,i}$, and the condition in the early stages of coagulation, $R_{ij}/2 = R_{c,i} = R_{c,j} = R_{H,i} = R_{H,j}$, both hold and a steady-state particle distribution is established (i.e.,

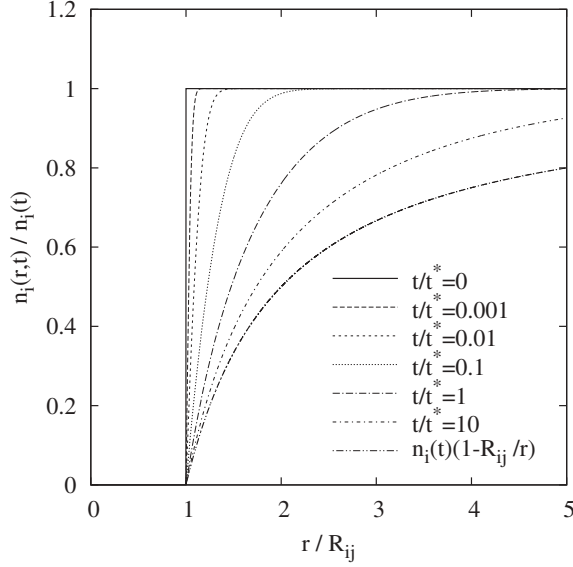


FIG. 1. The time dependence of particle spatial distribution is expressed by Eq. (2). Vertical and horizontal axes are normalized by $n_i(t)$ and R_{ij} , respectively. Particle distributions at $t/t^* = 0, 0.001, 0.01, 0.1, 1, 10$ are shown, where $t^* = R_{ij}^2/D_{ij}$. The steady-state particle distribution at $t/t^* \gg 1$ is also plotted.

$t \gg R_{ij}^2/D_{ij}$), Eq. (4) can be simplified as $\beta(i, j) = 2K^0 = 8k_B T/3\mu$. Here, k_B is the Boltzmann constant and T is the temperature. Furthermore, μ is the viscosity of the fluid, $R_{H,i}$ is the hydrodynamic radius of a cluster with size i , and $K^0 = 4k_B T/3\mu$ is the so-called Smoluchowski rate constant for rapid Brownian coagulation. Smoluchowski solved Eq. (1) for the early stages of the coagulation of an initially monodisperse, monomer suspensions. The total particle concentration, N_t , and the concentration of particles of each cluster size, n_i , are respectively given by

$$\frac{1}{N_t(t)} - \frac{1}{N_0} = Kt = \frac{t}{N_0 t_c}, \quad (5)$$

$$n_i(t) = N_0 \left(\frac{t}{t_c} \right)^{i-1} / \left(1 + \frac{t}{t_c} \right)^{i+1}, \quad (6)$$

where N_0 is the initial total particle concentration and the coefficient K on the right-hand side of Eq. (5) represents the coagulation rate in terms of the total number concentration. The index $i \geq 1$ in Eq. (6) represents the cluster size (number of particles in the cluster). For the ideal conditions proposed by Smoluchowski, $K = K^0$. The coagulation time t_c is defined as the time for the total particle concentration to decrease to half the initial particle concentration, $N_t(t_c) = N_0/2$. The time constant t_c represents a useful time scale for identifying the early stages of coagulation.

III. SIMULATION METHOD

We use a direct numerical scheme based on the SP method to consider the hydrodynamic many-body interaction between particles [24,29]. This method has been adapted to rheological studies and studies of the gelation of colloidal particle dispersions; it has been confirmed reasonably well [23,30]. In the present study, we consider the rapid Brownian

coagulation process for a system of monodisperse spherical particles in which the particles interact with one another through short-range attractive interactions.

We consider a monodisperse dispersion of N_p spherical particles with diameter $\sigma = 2a$ in a Newtonian host fluid, where a is the radius of a particle. The particles interact via a modified 200:100 Lennard-Jones potential as

$$V_{LJ}(r) = 4\epsilon[(\sigma/r)^{200} - (\sigma/r)^{100}], \quad (7)$$

where r is the distance between two particles and ϵ is the interaction strength. The large power index in Eq. (7) produces a short interaction range, corresponding to the rapid coagulation of sticky particles. In this study, the value of ϵ is fixed at $7.03k_B T$. This attractive potential strength is higher than the thermal fluctuation strength $k_B T$ and is sufficiently high to prevent coagulated particles from reversibly dispersing through thermal fluctuations.

The time evolution of particle i with mass $M_i = \pi\sigma^3\rho_p/6$ and moment of inertia I_i is governed by Newton's equations of motion as

$$M_i \dot{\mathbf{V}}_i = \mathbf{F}_i^H + \mathbf{F}_i^C + \mathbf{G}_i^V, \quad \dot{\mathbf{R}}_i = \mathbf{V}_i, \quad (8)$$

$$\mathbf{I}_i \cdot \dot{\boldsymbol{\Omega}}_i = \mathbf{N}_i^H + \mathbf{G}_i^\Omega, \quad (9)$$

where ρ_p is the density of the particle, \mathbf{R}_i is the position of the particle i , \mathbf{V}_i is the translational velocity of the particle, and $\boldsymbol{\Omega}_i$ is the rotational velocity of the particle. $\mathbf{F}_i^H, \mathbf{N}_i^H$ are the hydrodynamic forces and torques exerted by the fluid on each particle. \mathbf{F}_i^C is the interparticle force arising from the potential of Eq. (7). $\mathbf{G}_i^V, \mathbf{G}_i^\Omega$ are respectively random forces and torques due to thermal fluctuations. These random fluctuations are assumed to be Markovian and determine the temperature T . The procedure for determining the temperature is described in [31]. In the SP method, the velocity and pressure fields, $\mathbf{v}(\mathbf{x}, t)$ and $p(\mathbf{x}, t)$, are defined according to three-dimensional Cartesian grids that consist of fluid and particle domains. Each domain in the grids is distinguished by a smoothed function $\phi(\mathbf{x}, t)$, which is 1 in the particle domains and 0 in the fluid domains. These domains are separated by a thin interfacial domain of thickness ξ . The time evolution of the velocity field is governed by the Navier-Stokes equation with the incompressibility condition $\nabla \cdot \mathbf{v} = 0$ given by

$$\rho_f(\partial_t \mathbf{v} + \mathbf{v} \cdot \nabla \mathbf{v}) = -\nabla p + \mu \nabla^2 \mathbf{v} + \rho_f \phi \mathbf{f}_p, \quad (10)$$

where ρ_f is the density of the fluid and $\phi \mathbf{f}_p$ is the body force that ensures the rigidity of the particles and the appropriate non-slip boundary conditions at the fluid/particle interface. This phenomenon is explained in more detail elsewhere [24,29].

The unit of length in the lattice spacing is Δ ; the other fundamental units are μ and ρ_f . Similarly, the unit of time is $\tau = \rho_f \Delta^2 / \mu$ and the unit of energy is $\epsilon_0 = \Delta \mu^2 / \rho_f$. Unless otherwise stated, we set $\Delta = 1$, $\tau = 1$, $\mu = 1$, $\rho_f = 1$, $\rho_p = 1$, $a = 4$, $\sigma = 8$, $\xi = 2$, and the Lennard-Jones time unit $\tau_M = [(M_i \sigma^2) / \epsilon]^{1/2} \approx 131$. Assuming dispersions of neutrally buoyant particles of radius $1 \mu\text{m}$ in water at room temperature, our unit length Δ and time τ correspond to $0.25 \mu\text{m}$ and $0.0625 \mu\text{s}$. The second-order Runge-Kutta scheme is used to integrate Newton's equations. The Navier-Stokes equation is discretized by a Fourier spectral scheme in space and by a second-order Runge-Kutta scheme in time.

The discretized time step is $h = 0.07481$. Although this value is chosen from the stability condition of the Navier-Stokes equation, it is suitable for the particle equations because h is smaller than the period of the particle's vibration in the potential well $\tau_v = 2\pi[M_i/\dot{V}_{LJ}(2^{1/100}\sigma)]^{1/2} \approx 11.7$. Thus, a sufficiently short time step relative to the typical time scale for particle's motions is adopted.

IV. RESULTS AND DISCUSSION

The simulations were performed in a three-dimensional cubic box whose side length is L with periodic boundary conditions. All simulations assumed a constant volume system $L = 256$, where the number of particles was $N_p = 187, 281, 375, 625, 938, 1877, 3754$, and 6258. These conditions respectively correspond to $\phi_p = 0.003, 0.0045, 0.006, 0.01, 0.015, 0.03, 0.06$, and 0.1 where $\phi_p = \pi\sigma^3 N_p / 6L^3$. For spherical particles, $a = 4$ and $\xi = 2$. The thermal fluctuation forces on the particles are controlled for the temperature $k_B T / \epsilon_0 = 5.97$. The particle spatial distribution is initially random. To increase the statistical significance, five simulations were conducted for different random particle distributions. The total number of calculation steps is set to 25 000, which corresponds to 1874τ per calculation.

We employed the following criterion to determine aggregation of two particles. When the center-to-center distance of the particles is less than the threshold distance $R_{th} = 1.012\sigma$, the particle pair is included in the same cluster. As shown in Fig. 2, this threshold value corresponds to an interparticle distance where the potential energy is only $1.17k_B T$ higher than the minimum of the interparticle interaction potential V_{LJ} . The aggregates obtained consist of primary particles and form fractal structures at later stages of coagulation. One particle in

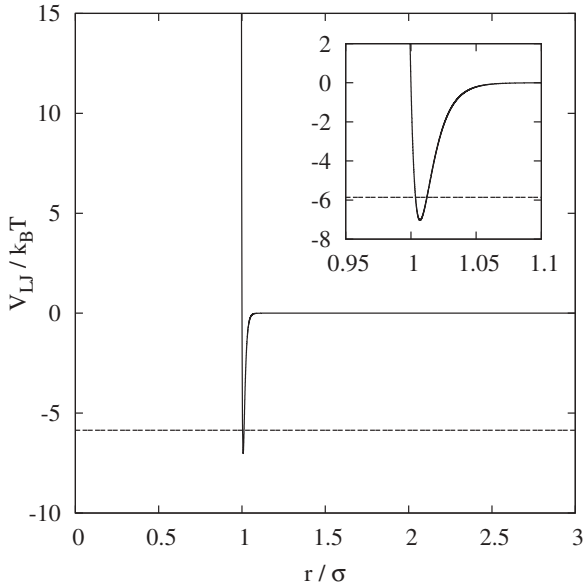


FIG. 2. Interparticle interaction potential. The particles interact via a modified 200:100 Lennard–Jones potential expressed by Eq. (7). The dashed line indicates an that is energy $1.17k_B T$ higher than the potential minimum. The inset shows an enlargement about $r/\sigma = 1$.

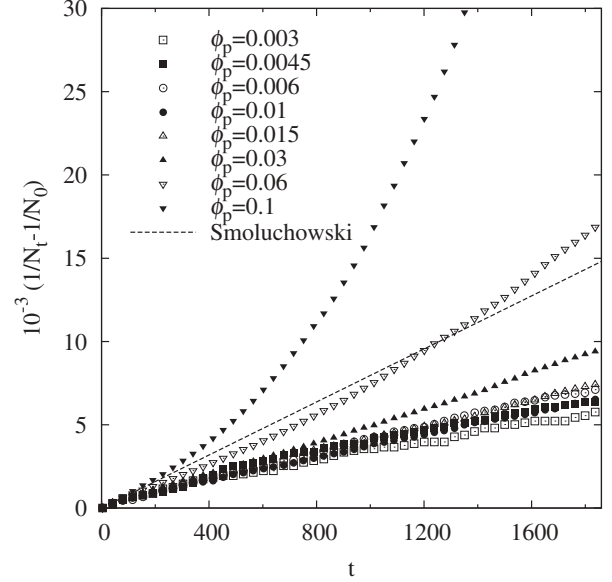


FIG. 3. Relation between $1/N_i(t) - 1/N_0$ and t . Dots represent the averages obtained for five different initial configurations. The dashed line shows the Smoluchowski theory given by Eq. (5), where $K = K^0 = 4k_B T / 3\mu$.

each doublet can rotate freely around the other, allowing for rearrangements of the cluster structure.

Figure 3 shows the temporal change of the reciprocal of the total particle concentration for different initial particle volume fractions. The slope represents the rate of coagulation. Smoluchowski's theoretical values are also plotted (dotted line) in this figure. The rapid coagulation rate given in Fig. 3 is less than the theoretical value predicted by Smoluchowski's theory for the dilute condition $\phi_p = 0.003$. Furthermore, increasing the volume fraction causes a corresponding increase in the slope of the plot in the early stages of aggregation. At higher volume fractions, $\phi_p \geq 0.03$, an additional, drastic increase in the slope is observed in the later stages of aggregation.

For similar experimental estimations of the coagulation rate at the early stages of coagulation [3], data in the time interval from $t = 0$ to t_c are used for least-squares fitting of the coagulation rate K by Eq. (5). For $\phi_p \leq 0.015$, the total particle number was not halved in the computed times and the fitting was performed over the whole data from the first time to the last. For $\phi_p = 0.03, 0.06, 0.1$, $t_c = 1745, 661, 288$, respectively. Figure 4 shows the volume fraction dependence of the ratio of the rate in the early stages of coagulation to Smoluchowski's coagulation rate K/K^0 . The ratio asymptotically approaches a certain value as it moves closer to the dilute limit volume fraction. The coagulation rate obtained is estimated to be approximately 0.3 to 0.5 times lower than that predicted by Smoluchowski for the dilute limit. This agrees relatively well with previous experimental results (e.g., the open point in Fig. 4) for which K/K^0 is reported to lie between 0.4 and 0.6 [2–6]. Nevertheless, our values are slightly lower than those obtained experimentally.

The deviation of the observed coagulation rate from Smoluchowski's theory can be mainly accounted for by the fact that Smoluchowski's theory does not consider interactions between

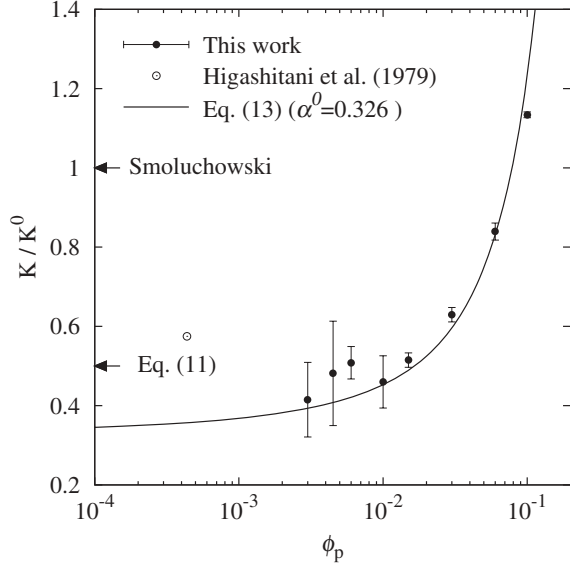


FIG. 4. Volume fraction dependence on the ratio of the coagulation rate K/K^0 . The coagulation rate K is obtained by fitting the data between $t = 0 \sim t_c$ with Eq. (5). The filled points represent calculated values in this study and the open point represents an experimental result of Higashitani *et al.* [4]. The arrows indicate Smoluchowski's result and $\alpha_{Br} = 0.5$ estimated by Eq. (11). The solid line represents Eq. (13).

particles. This theory ignores interparticle interactions, whereas attractive forces due to long-range Van der Waals-London potentials and repulsive forces due to HIs are known to greatly affect actual coagulation processes. The presence of these interactions necessitates corrections to Smoluchowski's theory. The effect on the interparticle potential $V(s)$ with respect to the coagulation rate was introduced as a stability factor by Fuchs, where $s = r/a$ [9]. Spielman then added the hydrodynamic lubrication effect between particles to the stability factor as a correction factor for the diffusion constant $C(s)$ [10]. According to their corrections, the ratio of the theoretical coagulation rate (including these interparticle interactions) to Smoluchowski's rate of rapid Brownian coagulation can be written as

$$\alpha_{Br} = K/K^0 = \left(2 \int_2^\infty \frac{C(s)}{s^2} e^{V(s)/k_B T} ds \right)^{-1}. \quad (11)$$

To calculate Eq. (11), Honig *et al.* used the Van der Waals attractive potential generated by Hamaker [32] and the approximate expressions for HIs in Eq. (12) as $V(s)$ and $C(s)$ in Eq. (11), respectively [11],

$$C(s) = (6s^2 - 11s)/(6s^2 - 20s + 16). \quad (12)$$

These authors reported that $\alpha_{Br} = 0.3$ – 0.6 , although this value varies depending on the strength of Van der Waals attractions. Their values are close to those obtained experimentally and the corresponding Hamaker constant agrees well with theoretical estimates [11]. Similar verifications have been conducted for a variety of particles and a variety of measurement techniques to verify the validity of the theoretical correction, according to Eq. (11) [4,6].

In our case, we estimated α_{Br} using Eqs. (7), (11), and (12), where the integral range in Eq. (11) is limited from

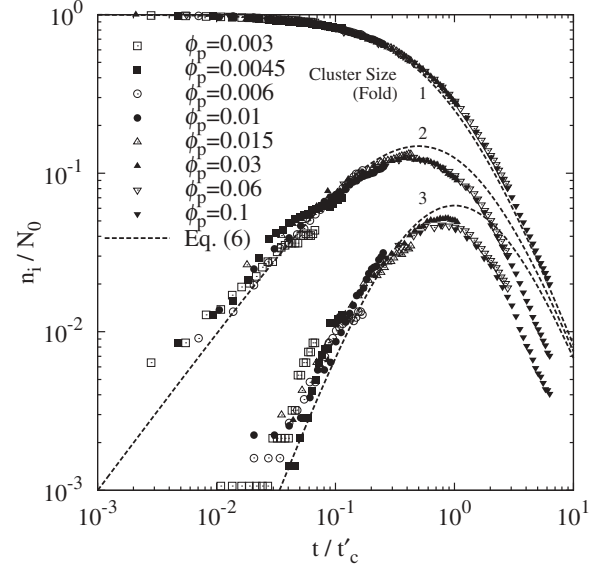


FIG. 5. Temporal concentration changes for particles of different sizes. Dots represent the results for up to a threefold cluster at $\phi_p = 0.01, 0.03, 0.1$. The horizontal axis is normalized by $t'_c = 1/KN_0$, as is expected from coagulation rates K . The dashed line indicates Eq. (6).

the distance of the Lennard-Jones potential minimum (i.e., $s = 2^{1/100}\sigma/a = 2.014$) to a sufficiently long distance. As indicated by the arrow in Fig. 4, the reduction in the coagulation rate due to interparticle interactions is estimated to be approximately 50% of Smoluchowski's value, which does not include interparticle interactions. The obtained α_{Br} corresponds reasonably well with the present numerical results for K/K^0 at lower volume fractions. The reduction in this estimated value relative to Smoluchowski's value is mainly due to the hydrodynamic lubrication effect, as represented by Eq. (12).

It should be emphasized that our simulation results with respect to the coagulation rate reduction from Smoluchowski's theoretical value are obtained by calculating HIs between particles without employing any approximations. Conventional studies that employ BD simulations often have discrepancies between experimental results and simulation-based results and the ratio of the coagulation rates K/K^0 is approximately unity due to HIs not being considered in the simulations. In contrast, our simulation results are consistent with current experimental and theoretical results, clearly indicating that HIs between particles play an important role in reducing the coagulation rate.

Furthermore, as shown in Fig. 4, increases in the volume fraction lead to gradual increases in the coagulation rate. This result is qualitatively consistent with experimental and simulation-based results [3,16,18,33]. The solid line shown in Fig. 4 is given by a formula based on the regression equation for the ratio of the coagulation rates K/K^0 in the high concentration system proposed by Heine *et al.* [16] as

$$K/K^0 = \alpha^0 \left(1 + \frac{2.5}{1 - \phi_p} (-\log \phi_p)^{-2.7} \right). \quad (13)$$

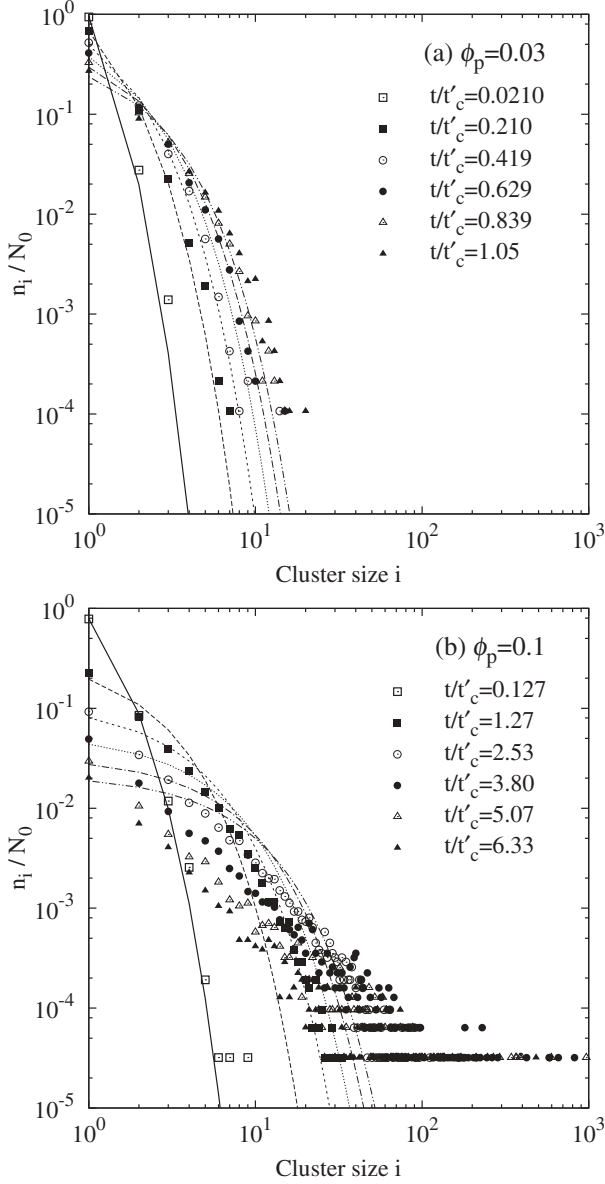


FIG. 6. Temporal variation of particle size distributions at (a) $\phi_p = 0.03$, (b) $\phi_p = 0.1$. Particle size distributions at $t/\tau = 37.48, 374.8, 749.6, 1124, 1499, 1874$ are shown. Time is normalized by t'_c . Lines indicate the lines of Eq. (6) calculated using the obtained coagulation rates K .

Because Heine *et al.* obtained this formula from the calculation results given by LD simulations in which HIs between particles are not considered, the prefactor $\alpha^0 = 1$ appears in their original formula. Their equation reduces to Smoluchowski's result $K/K^0 = 1$ in the dilute limit $(-\log \phi_p)^{-2.7} \ll 1$. We thus treat α^0 as the scaling factor. By least-squares fitting α^0 to our result, we obtained $\alpha^0 = 0.326$. This result agrees well with the form of Eq. (13) despite differences in the calculation methods for considering HIs. It thus seems that HIs directly affect the magnitude of the coagulation rate but they do not affect the dependence of the coagulation rate on the initial particle concentration for these relatively low volume fractions.

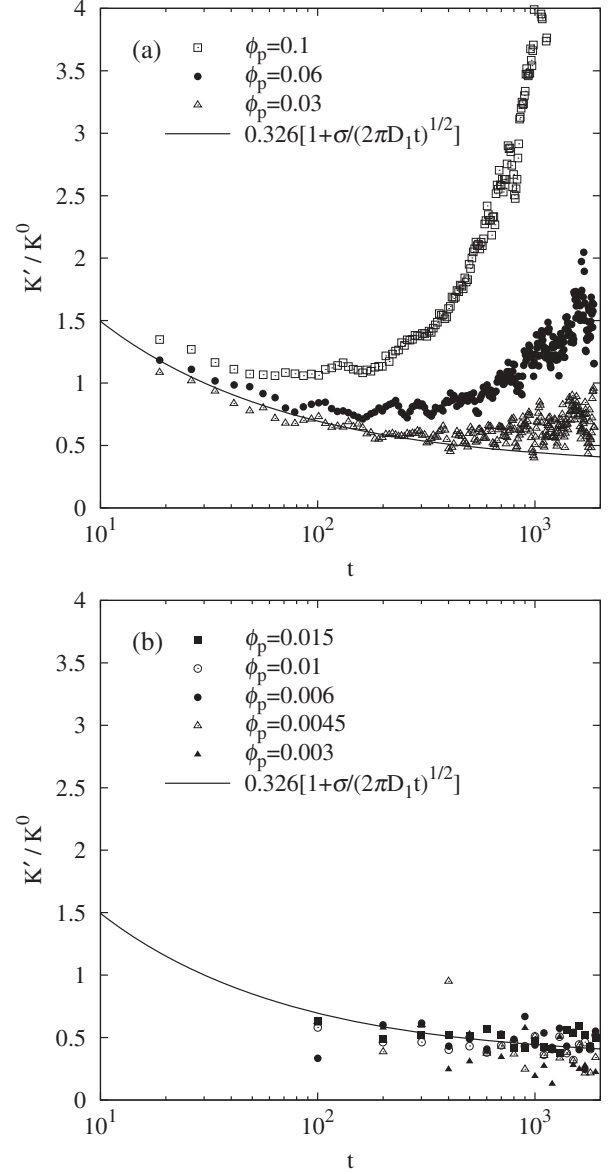


FIG. 7. Temporal variation of coagulation rate for (a) $\phi_p \geq 0.03$ and (b) $\phi_p < 0.03$. Temporal coagulation rate K' is obtained from the differential of $1/N_i$ at each time in Fig. 3. In (b), K' are averaged in time intervals of 100τ . The solid line indicates Smoluchowski's form for the coagulation rate, including unsteady-state effects [i.e., $\alpha^0(1 + R_{ij}/\sqrt{\pi D_{ij}t})$]. Here, the relationship $\alpha^0 = 0.326$, $R_{ij} = \sigma$, $D_{ij} = 2D_1 = 2k_B T/6\pi\mu a$ is assumed.

Figure 5 shows the relationship between cluster concentration and the size and time at each volume fraction. Time in the figure is normalized by the estimated coagulation time $t'_c = 1/K N_0$, where K is the coagulation rate obtained by the fitting. This figure also shows a theoretical line given by Eq. (6) in which t_c has been replaced with t'_c . As coagulation progresses, the number of primary particles decreases and the populations of doublet and triplet clusters increase. Next, the concentration of doublet and triplet clusters decreases after it reaches a maximum at around $t = t'_c$. In the early stages of coagulation (i.e., $t/t'_c < 1$), the concentration of each cluster size is in reasonable agreement with Eq. (6). However, in later stages

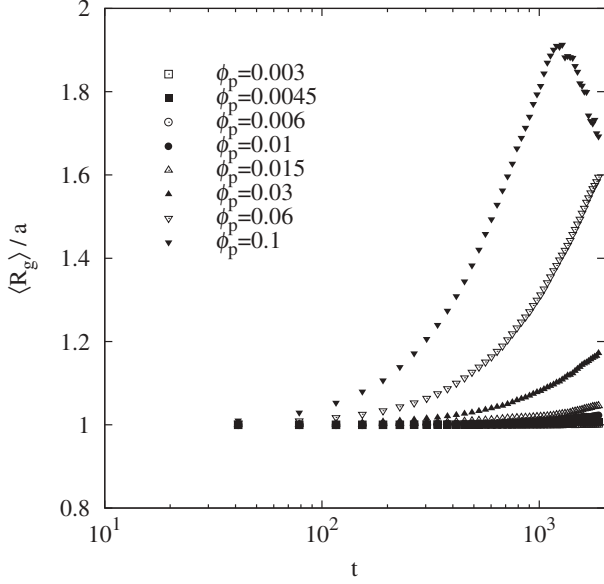


FIG. 8. Temporal variation of number average radius of gyration. Vertical axis is normalized by the primary particle's radius a . The averaging in Eq. (14) includes the contribution of primary particles assumed to be clusters with $R_g = a$.

of coagulation (i.e., $t/t'_c > 1$), especially for higher volume fractions $\phi_p \geq 0.03$, the concentration of doublet and triplet clusters falls significantly below the theoretical line. This result can be largely attributed to cluster-cluster or heterogeneous coagulation, as shown below. Figure 6 shows the temporal changes in the particle size distribution at $\phi_p = 0.03, 0.1$. The lines in the figure indicate Eq. (6) calculated using the obtained coagulation rates K . As seen in Fig. 5, data in the early stages of coagulation match Eq. (6) for a broad range of cluster sizes. However, in later stages of coagulation, the proportion of medium-sized clusters from twofold to several dozen fold decreases and larger clusters with sizes of several hundred fold are formed. These behaviors are thought to correspond to the drastic increase of the slope in the later stages of coagulation in Fig. 3. In this coagulation stage, coagulations between clusters with nonspherical bulky shapes or between clusters with heterogeneous collision diameters (e.g., between a large cluster and the small particles around it) [13,16] are observed in our simulations. At the end of the simulation of $\phi_p = 0.1$, a single large cluster expands to include the entire system, like in gelation (not shown).

As seen in our simulation results, the coagulation process at low particle volume fractions is still within the framework of Smoluchowski's assumptions until the end of the simulation runs. However, at higher particle volume fractions, our results show notable deviations from the early stage behavior. Next, we discuss briefly on the late stage behavior.

The time at which the coagulation rate is measured affects the coagulation rate and its volume fraction dependence. Figure 3 indicates that the gradient of $1/N_t$ temporally increases in the later stages of coagulation for high volume fractions. Figure 7 shows the temporal change in the coagulation rate, where the temporal coagulation rate K' is obtained from the difference between $1/N_t$ with respect to time, at a particular time in Fig. 3. At low volume fractions, short time changes of

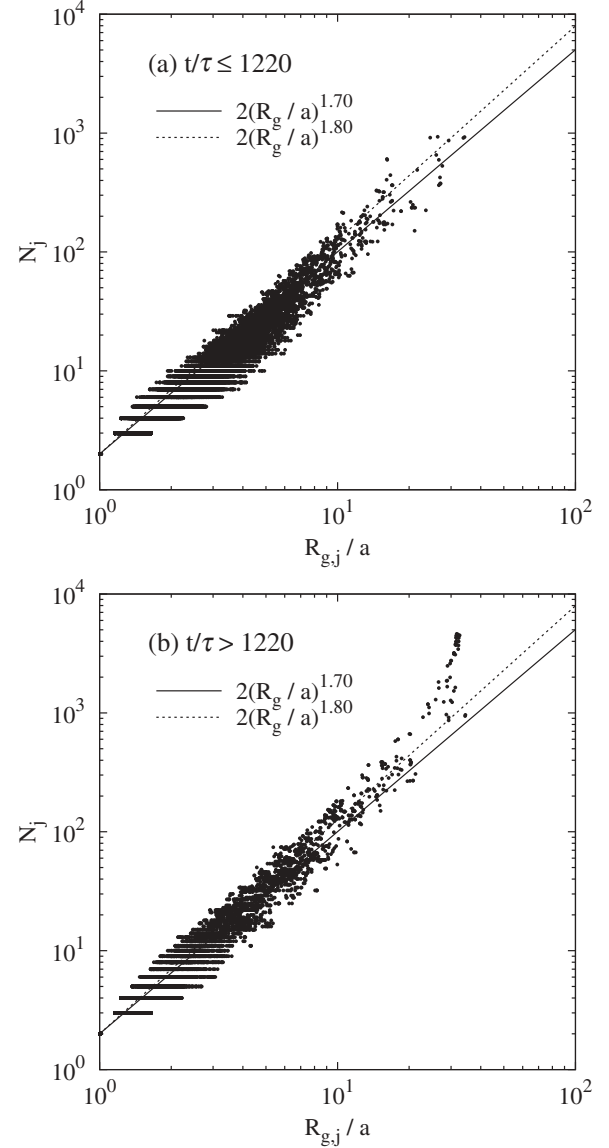


FIG. 9. The relationships between the cluster size N_i and the radius of gyration of cluster $R_{g,j}$ at $\phi_p = 0.1$ for (a) $t/\tau \leq 1220$ and (b) $t/\tau > 1220$. Equation (16) is shown by a solid line ($d_f = 1.7$) and a dashed line ($d_f = 1.8$).

$1/N_t$ are discrete due to the small numbers of particles, causing numerical differential of $1/N_t$ to vibrate largely. K' is thus averaged in time intervals of 100τ for $\phi_p < 0.03$ [Fig. 7(b)]. For $\phi_p \geq 0.03$ [Fig. 7(a)], the differentials are not averaged. The solid line in the figure represents Smoluchowski's expression for the coagulation rate, which includes unsteady-state effects, $\alpha^0(1 + R_{ij}/\sqrt{\pi D_{ij}t})$, like Eq. (4). Here, α^0 represents the ratio of the coagulation rate to that at steady state $t \gg R_{ij}^2/D_{ij}$. We chose α^0 as the same value obtained from the fitting of Eq. (13) in Fig. 4. The relationship $R_{ij} = \sigma, D_{ij} = 2D_1 = 2k_B T/6\pi\mu a$ is also assumed. In Fig. 7(a), the initial coagulation rate has a large value due to the unsteady-state particle spatial distribution, as shown in Fig. 1. As time progresses, the coagulation rate gradually decreases in a similar manner to Smoluchowski's form for the unsteady coagulation rate. The coagulation rate subsequently has a local minimum

at approximately $t = t_c$ and then increases abruptly due to the cluster-cluster or heterogeneous coagulations mentioned above. These minimum values in the temporal coagulation rate in Fig. 7 approximately correspond to the values of K/K^0 at $\phi_p \geq 0.03$ in Fig. 4. At $\phi_p < 0.03$, the coagulation rates tend to converge to constant values with time. In our case, the characteristic time constant for the unsteady-state regime is roughly estimated at $R_{ij}^2/D_{ij} \sim 12\pi\mu a^3/k_B T = 404\tau$. As the particle volume fraction increases, t_c becomes shorter and becomes comparable to this time constant. It is thus expected that at high particle volume fractions, the unsteady state in the initial coagulation stage will be immediately followed by the later cluster-cluster or heterogeneous coagulation process before the unsteady state converges.

Figure 8 shows the time evolution of the number average radius of gyration of clusters $\langle R_g \rangle$:

$$\langle R_g \rangle = \frac{1}{N_c} \sum_{j=1}^{N_c} R_{g,j}, \quad (14)$$

$$R_{g,j}^2 = \sum_{i=1}^{N_j} (\mathbf{R}_i^j - \mathbf{R}_{CM,j})^2 / N_j, \quad (15)$$

where N_c is the total number of clusters, N_j is the number of particles composing the j th cluster, \mathbf{R}_i^j is the position of the i th particle composing the j th cluster, and $R_{g,j}$ and $\mathbf{R}_{CM,j}$ are the radius of gyration and the center of mass of the j th cluster, respectively. The calculation of Eq. (14) includes primary particles assumed to be clusters with $R_g = a$. For $\phi_p \geq 0.03$, radiuses of gyration of clusters increase abruptly as time progresses. The time range for the growth in the radius of gyration reasonably corresponds to those for increases of coagulation rates in Fig. 7(a). This clearly suggests that spatial growth of clusters lead to increases of coagulation rate in the later stages of coagulation. At $\phi_p = 0.1$, the radius of gyration saturates and has a peak at about $t/\tau = 1220$. This reflects the generation of very large clusters expanding the whole of system as mentioned so far.

It is well known that the internal structure of colloidal aggregates and coagulation types can be described by concepts of fractal geometry. Several models and experimental results of

cluster growth for self-similar aggregates obey the following scaling relationship:

$$N_j \approx \left(\frac{R_{g,j}}{a} \right)^{d_f}, \quad (16)$$

where d_f is the fractal dimension which characterizes the cluster geometric structures [34–36]. Figure 9 indicates the relationship between cluster sizes and radiuses of gyration of clusters at $\phi_p = 0.1$. Figures 9(a) and 9(b) show data for $t/\tau \leq 1220$ and $t/\tau > 1220$, respectively. In the figure, lines of Eq. (16), in which a prefactor is fixed two from the relation that $R_g/\sigma = 2$ for doublets, are shown for comparison. In Fig. 9(a), plotted data almost follow the scaling relationship. However, in Fig. 9(b), points with large cluster sizes, $N_j \geq 1000$, deviate largely from the scaling relationship. This suggests the coexistence of very large clusters comparable to the system size with small ones. This was confirmed also by visualizations of cluster configurations.

V. CONCLUSIONS

The rate of rapid Brownian coagulation for fractional particle volume at dilute conditions $\phi_p = 0.003$ to that at high volume conditions $\phi_p = 0.1$ is investigated using the DNS method, which explicitly considers HIs between particles by simultaneously solving the motions of both the particles and the fluid. In the dilute cases, the rate of rapid Brownian coagulation is reduced to approximately 0.3–0.5 times the theoretical value predicted by Smoluchowski. This result is consistent with the results of previous experimental and theoretical studies that took account of hydrodynamic effects. Because exact HIs are explicitly incorporated in our simulation, the reproduction of this reduction in coagulation rate by our calculations clearly indicates that this observed reduction in the coagulation rate is caused by hydrodynamic effects. Moreover, the volume fraction dependence of the coagulation rate indicates that the coagulation rate increases with increasing volume fraction. At high particle volume fractions, the unsteady state in the initial coagulation stage is expected to be followed by a later, highly heterogeneous coagulation process before the unsteady state converges.

-
- [1] M. Smoluchowski, *Z. Phys. Chem., Stochiom. Verwandtschaftsl* **92**, 129 (1917).
 [2] J. W. T. Lichtenbelt, C. Pathmanoharan, and P. H. Wiersema, *J. Colloid Interface Sci.* **49**, 281 (1974).
 [3] W. Hatton, P. Mcfadyen, and A. L. Smith, *J. Chem. Soc., Faraday Trans. 1* **70**, 655 (1974).
 [4] K. Higashitani and Y. Matsuno, *J. Chem. Eng. Jpn.* **12**, 460 (1979).
 [5] H. Sonntag and K. Strenge, *Coagulation Kinetics and Structure Formation* (Plenum, New York, 1987).
 [6] H. Holthoff, S. U. Egelhaaf, M. Borkovec, P. Schurtenberger, and H. Sticher, *Langmuir* **12**, 5541 (1996).
 [7] B. V. Deryaguin and L. Landau, *Acta Phys. Chem.* **14**, 633 (1941).
 [8] E. J. W. Verwey and J. T. G. Overbeek, *Theory of the Stability of Lyophobic Colloids* (Elsevier, Amsterdam, 1948).
 [9] N. Fuchs, *Z. Phys.* **87**, 736 (1934).
 [10] L. A. Spielman, *J. Colloid Interface Sci.* **33**, 562 (1970).
 [11] E. P. Honig, G. J. Roeberson, and P. H. Wiersema, *J. Colloid Interface Sci.* **36**, 97 (1971).
 [12] K. Higashitani, T. Tanaka, and Y. Matsuno, *J. Colloid Interface Sci.* **63**, 551 (1978).
 [13] T. Fukasawa and Y. Adachi, *J. Colloid Interface Sci.* **304**, 115 (2006).

- [14] Y. Kusaka, T. Fukasawa, and Y. Adachi, *J. Colloid Interface Sci.* **363**, 34 (2011).
- [15] G. J. Roeberson and P. H. Wiersema, *J. Colloid Interface Sci.* **49**, 98 (1974).
- [16] M. C. Heine and S. E. Pratsinis, *Langmuir* **23**, 9882 (2007).
- [17] B. Buesser, M. C. Heine, and S. E. Pratsinis, *Aerosol Sci.* **40**, 89 (2009).
- [18] G. Urbina-Villalba, J. Toro-Mendoza, A. Lozsán, and M. García-Sucre, *J. Phys. Chem. B* **108**, 5416 (2004).
- [19] M. Lattuada, *J. Phys. Chem. B* **116**, 120 (2012).
- [20] J. F. Brady and G. Bossis, *Annu. Rev. Fluid Mech.* **20**, 111 (1988).
- [21] D. R. Foss and J. F. Brady, *J. Fluid Mech.* **407**, 167 (2000).
- [22] H. Tanaka and T. Araki, *Phys. Rev. Lett.* **85**, 1338 (2000).
- [23] R. Yamamoto, K. Kim, Y. Nakayama, K. Miyazaki, and D. R. Reichman, *J. Phys. Soc. Jpn.* **77**, 084804 (2008).
- [24] Y. Nakayama and R. Yamamoto, *Phys. Rev. E* **71**, 036707 (2005).
- [25] J. T. Padding and A. A. Louis, *Phys. Rev. E* **74**, 031402 (2006).
- [26] M. Fujita and Y. Yamaguchi, *Phys. Rev. E* **77**, 026706 (2008).
- [27] I. Pagonabarraga, B. Rotenberg, and D. Frenkel, *Phys.Chem.Chem.Phys.* **12**, 9566 (2010).
- [28] S. A. Rice, in *Diffusion-Limited Reactions*, Compr. Chem. Kinetics 25, edited by C. H. Bamford, C. F. H. Tipper, and R. G. Compton (Elsevier, Amsterdam, 1985).
- [29] Y. Nakayama, K. Kim, and R. Yamamoto, *Eur. Phys. J. E* **26**, 361 (2008).
- [30] T. Iwashita and R. Yamamoto, *Phys. Rev. E* **80**, 061402 (2009).
- [31] T. Iwashita, Y. Nakayama, and R. Yamamoto, *J. Phys. Soc. Jpn.* **77**, 074007 (2008).
- [32] H. C. Hamaker, *Physica* **4**, 1058 (1937).
- [33] T. M. Trzeciak, A. Podgóski, and J. C. M. Marijnissen, in *Proceedings of the Fifth World Congress on Particle Technology* (Orlando, FL, USA, 2006), p. 202d.
- [34] R. Jullien, M. Kolb, and R. Botet, *J. Phys. (Paris), Lett.* **45**, L977 (1984).
- [35] D. A. Weitz, J. S. Huang, M. Y. Lin, and J. Sung, *Phys. Rev. Lett.* **54**, 1416 (1985).
- [36] M. Y. Lin, H. M. Lindsay, D. A. Weitz, R. Klein, R. C. Ball, and P. Meakin, *J. Phys.: Condens. Matter* **2**, 3093 (1990).